Eur. Phys. J. A (2012) **48**: 13
DOI 10.1140/epja/i2012-12013-x

THE EUROPEAN PHYSICAL JOURNAL A

Regular Article – Experimental Physics

New determination of the astrophysical $^{13}C(p,\gamma)^{14}N$ S(E) factors and reaction rates via the $^{13}C(^7Li, ^6He)^{14}N$ reaction

Y.J. Li[1], Z.H. Li[1,a], E.T. Li[1], X.X. Bai[1], J. Su[1], B. Guo[1], B.X. Wang[1], S.Q. Yan[1], S. Zeng[1], Z.C. Li[1], J.C. Liu[1], X. Liu[1], S.J. Jin[1], Y.B. Wang[1], L.Y. Zhang[2], X.Q. Yu[2], L. Li[2], G. Lian[1], Q.W. Fan[1], and W.P. Liu[1]

[1] China Institute of Atomic Energy (CIAE), P. O. Box 275(10), Beijing 102413, PRC
[2] Institute of Modern Physics, Chinese Academy of Sciences (CAS), Lanzhou 730000, PRC

Received: 23 October 2011 / Revised: 8 January 2012
Published online: 9 February 2012 –
Communicated by H. Miyatake

Abstract. The $^{13}C(^7Li,^6He)^{14}N_{0,1}$ reactions were measured at $E(^7Li) = 34$ MeV with the Q3D magnetic spectrometer of the HI-13 tandem accelerator, and the first peaks of the angular distributions were obtained for the first time. The $^{14}N_{0,1}$ proton spectroscopic factors were extracted to be 0.67 ± 0.09 and 0.73 ± 0.10, respectively. Using the $^{13}C(p,\gamma)^{14}N$ direct capture $S_{dc}(E)$ factors derived by the spectroscopic factors, the direct measurement data for both 1^- and 0^- resonances were well fitted via updating the resonance parameters, and then the total astrophysical $^{13}C(p,\gamma)^{14}N$ $S(E)$ factors and reaction rates were determined at stellar energies. The present work offers an independent examination to the existing results of the $^{13}C(p,\gamma)^{14}N$ reaction.

1 Introduction

$^{13}C(p,\gamma)^{14}N$ is one of the key reactions in the CNO cycle [1]. Its astrophysical reaction rates directly affect the ^{13}C abundance and hence the ratio of ^{12}C to ^{13}C. This reaction may also affect to some extent the *s*-process nucleosynthesis because it destroys the seed nuclei of the $^{13}C(\alpha,n)^{16}O$ neutron source reaction for AGB stars with solar metalicity [2], even though the amount of ^{13}C is usually believed to be dominated by the slower $^{12}C(p,\gamma)^{13}N$ rate.

So far, several direct measurements of the $^{13}C(p,\gamma)^{14}N$ reaction [3–6] have only reached down to 100 keV which is much higher than the stellar energies (~ 25 keV). The accurate measurement for the $S(E)$ factors was carried out in the energy range of 100–900 keV [6], and the *R*-matrix fit gave $S(0) = 7.6$ keV b [7,8], whereas the latest measurement in inverse kinematics and *R*-matrix fit deduced a relatively small result of $S(0) = 4.85$ keV b [9].

There are two excited states at 1^-8062 keV and 0^-8776 keV in ^{14}N contribute to the $^{13}C(p,\gamma)^{14}N$ resonant captures in the astrophysical energy region. Although the contribution from the resonance tails may be much higher than that from the direct capture component, the interference between two processes can lead to an appreciable influence on the total $S(E)$ factors. Thus the precise measurement of direct capture is necessary to obtain the reliable $S(E)$ factors, particularly at astrophysically relevant energies. The $^{13}C(p,\gamma)^{14}N$ direct capture cross-section can be derived in term of spectroscopic factor or asymptotic normalization coefficient (ANC) of $^{14}N \rightarrow {}^{13}C + p$, deduced from the angular distribution of proton transfer reactions.

Several experiments have been performed to study the spectroscopic factors or ANCs of $^{14}N \rightarrow {}^{13}C + p$ through the $^{13}C(d, n)$ [10,11], $^{13}C(^3He, d)$ [12–14], $^{13}C(^7Li,^6He)$ [15] and $^{13}C(^{14}N,^{13}C)$ [16] reactions. The spectroscopic factors and ANCs extracted from these measurements deviate in varying degrees, especially for the first excited state in ^{14}N. In order to clarify the discrepancy, new measurement is still needed. The $(^7Li,^6He)$ reactions are thought to be a valuable spectroscopic tool [17] because the shapes of their angular distributions can be well reproduced by the distorted wave Born approximation (DWBA), and the proton spectroscopic factor of ^7Li is well determined [18,19]. Unfortunately, the abovementioned $^{13}C(^7Li,^6He)$ measurement missed the first peak of angular distribution. Hence it is highly desired to ameliorate the measurement of $^{13}C(^7Li, ^6He)^{14}N$ reaction.

In the present work, the angular distributions of ^7Li elastic scattering on ^{13}C and $^{13}C(^7Li,^6He)^{14}N$ transfer reactions leading to ground and first excited states in ^{14}N have been measured with the Q3D magnetic spectrometer [20] at $E(^7Li) = 34$ MeV. The spectroscopic factors were derived based on DWBA analysis, and then used to calculate the astrophysical $^{13}C(p,\gamma)^{14}N$ $S(E)$ factors and reaction rates at stellar energies.

[a] e-mail: zhli@ciae.ac.cn

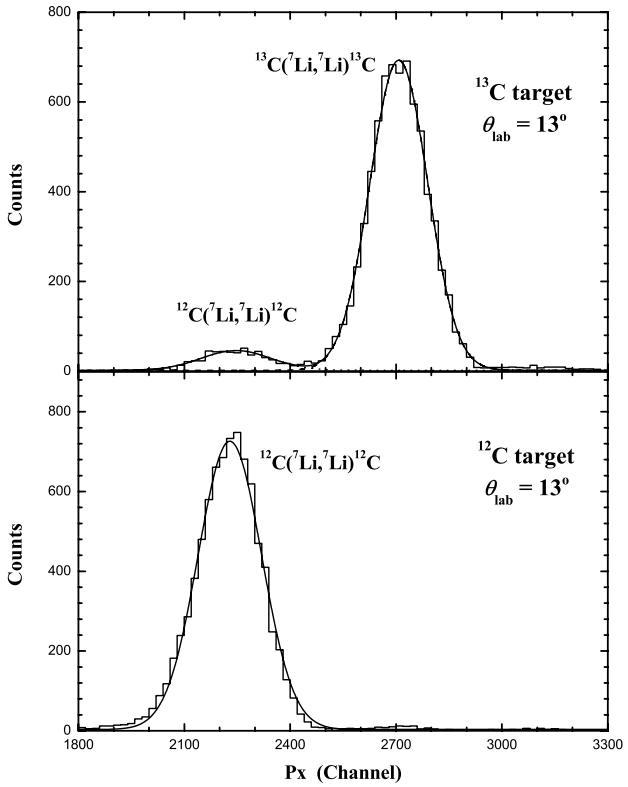

Fig. 1. Typical position spectra on the Q3D focal plane for the ^{7}Li + ^{12,13}C elastic scattering.

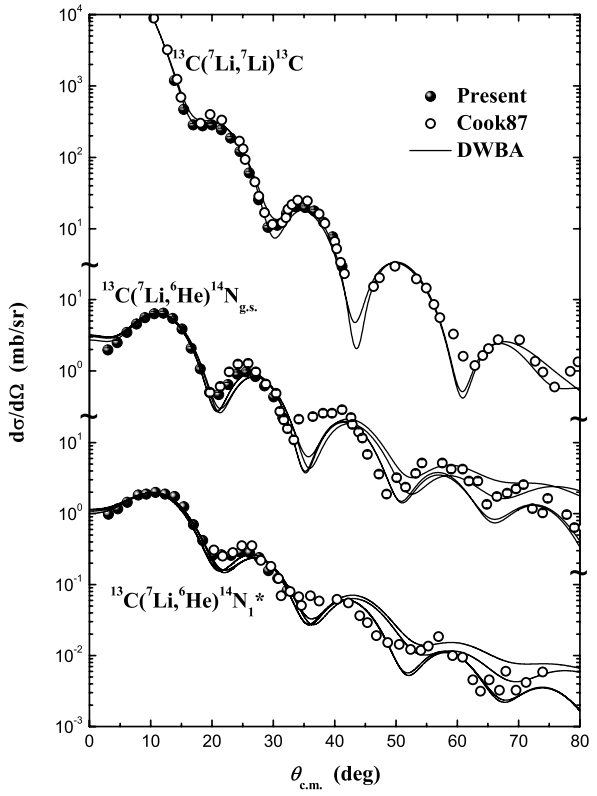

Fig. 2. Angular distributions of ^{13}C(^{7}Li, ^{7}Li)^{13}C, ^{13}C(^{7}Li, ^{6}He)^{14}N$_0$ and ^{13}C(^{7}Li, ^{6}He)^{14}N$_1^*$ at $E(^7\text{Li}) = 34$ MeV, together with the DWBA calculations. The solid and open circles denote the data obtained in the present experiment and the earlier work [15], respectively.

2 Measurement of the angular distributions

Our experiment was carried out with a 34 MeV ^{7}Li beam from the HI-13 tandem accelerator, Beijing. The 150 enA ^{7}Li beam impinged on a 90 μg/cm^2 self-supporting ^{13}C target with a purity of 94%. A ^{12}C target with the same thickness served as the background measurement. A removable Faraday cup behind the target was used to collect the beam for normalization. It covered an angular range of $\pm 6°$ and thus restricted the attainable minimum angle. The relative normalization of measurements at angles of $\theta_{\text{lab}} \leq 6°$ was carried out by monitoring the elastic scattering events with a ΔE-E counter telescope placed at 25° downstream of the target. The accepted solid angle of Q3D magnetic spectrometer was set to be 0.34 mSr for a good angular resolution. The reaction products were focused and separated by Q3D, and measured by a 50 mm × 50 mm two-dimensional position sensitive silicon detector (PSSD) on the focal plane.

The ^{13}C(^{7}Li,^{7}Li)^{13}C elastic scattering and the ^{13}C(^{7}Li, ^{6}He)^{14}N$_{0,1}$ transfer reactions were measured in the angular ranges of $9° \leq \theta_{\text{lab}} \leq 27°$ and $2° \leq \theta_{\text{lab}} \leq 21°$ in steps of 1°, respectively. The typical position spectra of elastic scattering events for ^{7}Li on ^{13}C and ^{12}C targets are shown in fig. 1. The purity of ^{13}C target can be determined accurately via the analysis of the position spectra. The disturbance from the ^{12}C contaminant in ^{13}C target can completely be eliminated based on the position spectra at each angle. Finally, the ^{13}C(^{7}Li,^{7}Li)^{13}C, ^{13}C(^{7}Li,^{6}He)^{14}N$_0$ and ^{13}C(^{7}Li,^{6}He)^{14}N$_1^*$ angular distributions were obtained as shown in fig. 2 with solid circles. It can be seen clearly that the first peaks of ^{13}C(^{7}Li,^{6}He)^{14}N$_{0,1}$ angular distributions are fully measured in the present work. The uncertainties of the differential cross-sections are about 7%, mainly from the statistics and ununiformity of the target thickness.

3 DWBA calculations

^{13}C(^{7}Li,^{6}He)^{14}N$_{0,1}$ angular distributions were calculated with the DWBA code PTOLEMY [21]. The optical potential parameters for the entrance channel were chosen from ref. [15] and extracted by fitting the present ^{13}C(^{7}Li, ^{7}Li)^{13}C angular distribution with real and imaginary potentials of Woods-Saxon form, respectively. Since no experimental data exist for the ^{6}He elastic scattering on ^{14}N, the angular distributions of the ^{14}N(^{6}Li,^{6}Li)^{14}N at $E(^6\text{Li}) = 32$ MeV [22] and ^{13}C(^{6}Li,^{6}Li)^{13}C at $E(^6\text{Li}) = 28$ MeV [23] were used to derive the potential parameters for the exit channels. All the potential parameters are listed in table 1. For calculating the wave functions of the bound states, the Woods-Saxon potentials with the standard geometrical parameters $r_0 = 1.25$ fm and $a = 0.65$ fm were adopted, and the potential depths were adjusted automatically to reproduce the proton binding energies of ^{14}N$_{0,1}$.

Table 1. Woods-Saxon potential parameters for the entrance and exit channels of ^{13}C(^{7}Li,^{6}He)^{14}N$_{0,1}$. Set I is taken from ref. [15], Set Ⅱ, Ⅲ and Ⅳ are extracted by fitting the ^{13}C(^{7}Li,^{7}Li)^{13}C, ^{14}N(^{6}Li,^{6}Li)^{14}N and ^{13}C(^{6}Li,^{6}Li)^{13}C elastic scattering angular distributions, respectively. The depths and geometrical parameters are in MeV and fm, respectively. The last row gives the goodness of fit(χ^2 per point).

Channel	^{7}Li + ^{13}C		^{6}He + ^{14}N	
	Set I	Set Ⅱ	Set Ⅲ	Set Ⅳ
U_V	159.0	198.75	124.88	131.65
r_R	0.63	0.52	0.52	0.60
a_R	0.81	0.90	1.02	0.91
W_V	8.16	8.70	15.37	7.14
r_I	1.33	1.31	1.30	1.31
a_I	0.78	0.73	0.54	0.7
r_C	1.25	1.0	1.0	1.0
χ^2/p		15.22	6.37	1.35

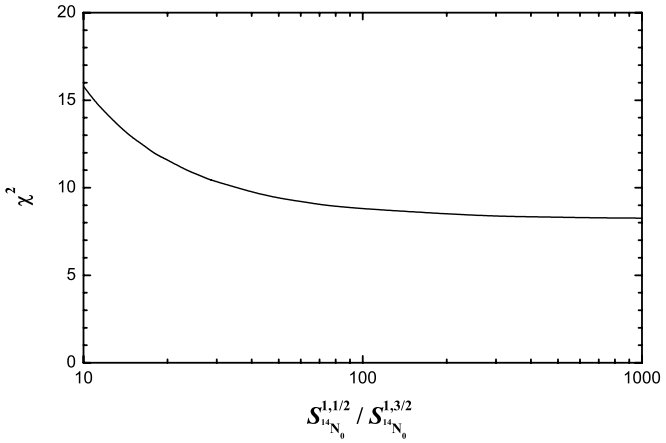

Fig. 3. Goodness of fit *vs.* $S_{p1/2}/S_{p3/2}$ for the ^{13}C(^{7}Li, ^{6}He)^{14}N$_0$ angular distribution.

The ^{14}N proton spectroscopic factor $S^{l_pj_p}_{^{14}\mathrm{N}}$ can be derived by normalizing the DWBA calculations to the experimental data according to the expression

$$\left(\frac{\mathrm{d}\sigma}{\mathrm{d}\Omega}\right)_{\mathrm{exp}} = \sum_{l_pj_p} S_{^7\mathrm{Li}} S^{l_pj_p}_{^{14}\mathrm{N}} \left(\frac{\mathrm{d}\sigma}{\mathrm{d}\Omega}\right)^{l_pj_p}_{\mathrm{DWBA}}, \quad (1)$$

where $(\mathrm{d}\sigma/\mathrm{d}\Omega)_{\mathrm{exp}}$ and $(\mathrm{d}\sigma/\mathrm{d}\Omega)_{\mathrm{DWBA}}$ are the measured and calculated differential cross-sections, respectively. The proton spectroscopic factor of ^{7}Li has been determined to be $S_{^7\mathrm{Li}} = 0.42$ in refs. [18,19].

Proton transfers to the $1p_{1/2}$ and $1p_{3/2}$ orbits of the ground state in ^{14}N were taken into account in the analysis of experimental data. It was found that the χ^2 decreases with the increase of $S^{1,1/2}_{^{14}\mathrm{N}_0}/S^{1,3/2}_{^{14}\mathrm{N}_0}$, as shown in fig. 3. This result indicates that $S^{1,1/2}_{^{14}\mathrm{N}_0}/S^{1,3/2}_{^{14}\mathrm{N}_0}$ should be greater than 100 according to the precision of our experiment. It supports the theoretical calculations [24,25], and differs from the previously experimental value of 20 [16]. Because of the very small contribution, the $1p_{3/2}$ component was neglected in DWBA analysis for the ^{13}C(^{7}Li,^{6}He)^{14}N$_0$ reaction. For the proton transfer to the first exited state in ^{14}N, only $1p_{1/2}$ component was taken into account due to the parity and angular momentum constraints.

Table 2. Theoretical and experimental proton spectroscopic factors for the ground and first exited states in ^{14}N.

$S_{^{14}N_0}$	$S_{^{14}N^*_1}$	Exp. or The.	Ref.
0.68	0.99	Theory	[24]
0.80	0.96	Theory	[26]
0.65	0.89	Theory	[27]
1.09±0.19	1.42±0.24	^{13}C(d, n)^{14}N	[10]
0.50±0.10	0.56±0.11	^{13}C(d, n)^{14}N	[11]
0.76±0.15	0.92±0.18	^{13}C(^{3}He,d)^{14}N	[12]
0.58±0.04	0.93±0.07	^{13}C(^{3}He,d)^{14}N	[13]
0.60±0.09	0.79±0.12	^{13}C(^{3}He,d)^{14}N	[14]
0.68±0.04	0.58±0.06	^{13}C(^{14}N,^{13}C)^{14}N	[16]
0.62±0.07	0.83±0.10	^{13}C(^{7}Li,^{6}He)^{14}N	[15]
0.67±0.09	0.73±0.10	^{13}C(^{7}Li,^{6}He)^{14}N	Present Work

The calculated results are also shown in fig. 2 with solid lines. It can be seen that the experimental angular distributions are well reproduced. Differently from the earlier (^{7}Li,^{6}He) study [15], no obvious phase shift between the calculations and the experimental data is found in the present work. The spectroscopic factors of $^{14}\mathrm{N}_0 \rightarrow {}^{13}\mathrm{C} + p$ and $^{14}\mathrm{N}^*_1 \rightarrow {}^{13}\mathrm{C} + p$ are determined to be 0.67±0.09 and 0.73±0.10, respectively. The uncertainties are mainly from the measurement (7%), divergence of optical potential parameters (8%) and error of the ^{7}Li proton spectroscopic factors (9%). The spectroscopic factors obtained in several theoretical and experimental investigations are listed in table 2. Our result is in fair agreement with those derived from the ^{13}C(^{3}He, d)^{14}N [14] and ^{13}C(^{14}N,^{13}C)^{14}N [16] reactions within the uncertainty. As compared to the previous ^{13}C(^{7}Li, ^{6}He)^{14}N work [15], the results are close to each other by chance, however, the $S_{^7\mathrm{Li}}$ cited therein is a factor of 1.4 larger than that used in our calculations.

4 The astrophysical ^{13}C(p, γ) S(E) factors and reaction rates

The ^{13}C$(p,\gamma)^{14}$N direct captures are dominated by the $E1$ transition from incoming s-, d-wave to the first three bound states and p-wave to the next four excited states in ^{14}N. The astrophysical $S(E)$ factors are related to the cross-sections by

$$S(E) = E\sigma(E)\exp(2\pi\eta), \quad (2)$$

where E is the relative kinetic energy, $\eta = Z_1Z_2\mu/k$ stands for the Coulomb parameter in the initial state, μ and k denote the reduced mass and the wave number. The cross-

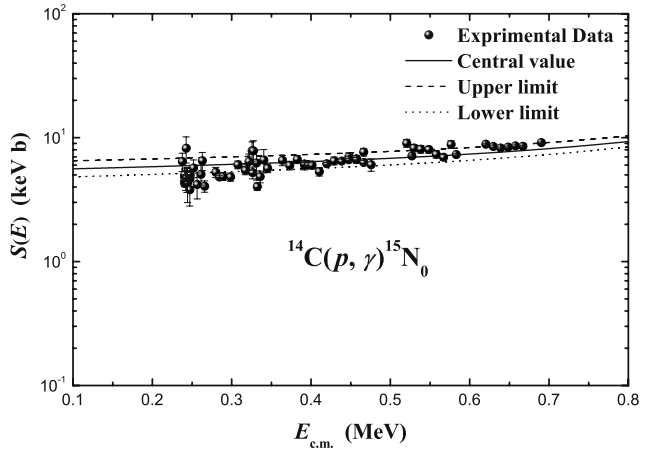

Fig. 4. Astrophysical $S(E)$ factors for the $^{14}\mathrm{C}(p,\gamma)^{15}\mathrm{N}_0$ reaction. The solid circles denote the experimental data from [33]. The solid, dashed and dotted lines are central value, upper and lower limits, respectively.

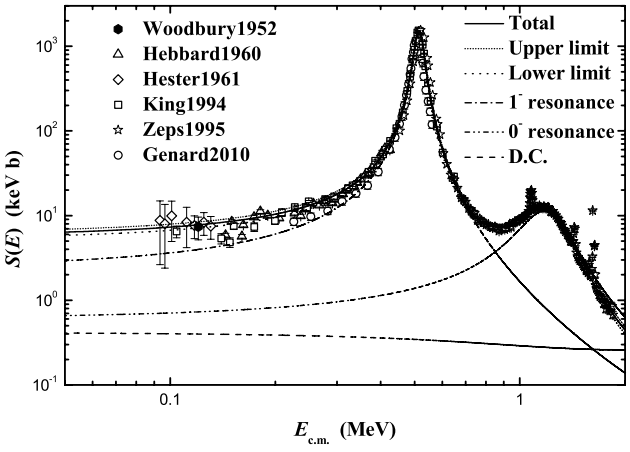

Fig. 5. Astrophysical $^{13}\mathrm{C}(p,\gamma)^{14}\mathrm{N}_0$ $S(E)$ factors. The experimental data are taken from refs. [3–6,9,38]. The various lines are the calculated results in the present work.

section for $E1$ direct capture can be expressed as [28,29]

$$\sigma = \frac{16\pi}{9}\left(\frac{E_\gamma}{\hbar c}\right)^3 \frac{e_{\mathrm{eff}}^2}{k^2}\frac{1}{\hbar v}\frac{(2I_f+1)}{(2I_1+1)(2I_2+1)}S_{l_f j_f} \times \left|\int_0^\infty r^2 \omega_{l_i}(kr) u_{l_f}(r)\mathrm{d}r\right|^2, \quad (3)$$

where E_γ is the γ-ray energy; k denotes the incident wave number; $e_{\mathrm{eff}} = e(A-Z)/(A+1)$ stands for the proton effective charge of the $E1$ transition in the potential produced by a target nucleus with mass number A and atomic number Z; v is the relative velocity between proton and ^{13}C; I_1, I_2 and I_f are the spins of proton, ^{13}C, and ^{14}N, respectively; $S_{l_f j_f}$ is the proton spectroscopic factor of ^{14}N; $\omega_{l_i}(kr)$ is the distorted radial wave function for the entrance channel, and $u_{l_f}(r)$ is the radial wave function of the bound state proton in ^{14}N.

In the calculation of $\omega_{l_i}(kr)$, the imaginary part of the optical potential was neglected because of the small flux into other reaction channels. For the real part, a Wood-Saxon potential is adopted, for which r_0 and a were set as the same as those for the $^{14}\mathrm{N}\rightarrow{}^{13}\mathrm{C} + p$ bound state. According to the previous approach [28,30–32], the potential depth for the $^{13}\mathrm{C} + p$ system was adjusted to reproduce the volume integral of potential per nucleon $J_\mathrm{V}/A = 334 \pm 12\,\mathrm{MeV\,fm^3}$ derived from fit the astrophysical $^{14}\mathrm{C}(p,\gamma)^{15}\mathrm{N}_0$ $S(E)$ factors [33]. The same proton spectroscopic factor of $^{15}\mathrm{N}_0$ and resonance parameters as adopted in ref. [33] were used in our fitting, the result is shown in fig. 4. With the fitted J_V/A value, the $^{13}\mathrm{C} + p$ potential depth was derived to be $V_0 = 27.5 \pm 1.0\,\mathrm{MeV}$. Based on the $S_{^{14}\mathrm{N}}$ and potential parameters derived above, the energy dependence of astrophysical $^{13}\mathrm{C}(p,\gamma)^{14}\mathrm{N}_0$ direct capture $S_{\mathrm{dc}}(E)$ factors was calculated as shown in fig. 5 with dashed line.

The resonant capture $S_{\mathrm{res}}(E)$ factors can be calculated with the Breit-Wigner formula [1],

$$S_{\mathrm{res}}(E) = \frac{\pi\hbar^2}{2\mu}\frac{2J+1}{(2J_1+1)(2J_2+1)} \times \frac{\Gamma_p(E)\Gamma_\gamma(E)}{(E-E_R)^2+(\Gamma_{\mathrm{tot}}/2)^2}\exp(2\pi\eta), \quad (4)$$

where J, J_1 and J_2 are the spins of ^{14}N, proton and ^{13}C, respectively; E_R stands for the resonance energy; Γ_p, Γ_γ and Γ_{tot} denote the proton, radiative and total widths in sequence. The energy dependence of Γ_p and Γ_γ are given by [34]

$$\Gamma_{p,l}(E) = \frac{P_l(E)}{P_l(E_\mathrm{R})}\Gamma_{p,l}(E_\mathrm{R}), \quad (5)$$

and

$$\Gamma_\gamma(E) = \left(\frac{E+\varepsilon_f}{E_\mathrm{R}+\varepsilon_f}\right)^{2L+1}\Gamma_\gamma(E_\mathrm{R}), \quad (6)$$

where $\Gamma_p(E_\mathrm{R})$ and $\Gamma_\gamma(E_\mathrm{R})$ are the experimental partial and radiative widths; l, L and ε_f donate the orbital angular momentum, multipolarity of the gamma transition and the proton binding energy of the bound state in residual nucleus, respectively. The penetrability $P_l(E)$ is given by

$$P_l(E) = \frac{ka}{F_l^2(k,a)+G_l^2(k,a)}, \quad (7)$$

where F_l and G_l are the regular and singular solutions of the radial Schrödinger equation, and a is the channel radius.

The function used to fit the total $S(E)$ factors is [35,6]

$$S(E) = S_{\mathrm{dc}}(E) + \sum_i S_{\mathrm{res}i}(E) \pm \sum_i 2\left[S_{\mathrm{dc}}(E)S_{\mathrm{res}i}(E)\right]^{1/2}\cos(\delta_i), \quad (8)$$

Table 3. Resonance parameters for the $^{13}C(p,\gamma)^{14}N$ reaction.

	E_R (keV)			
J^π, T	Ref. [6]	Ref. [38]	Ref. [8]	Present
1^-, 1	518.14±0.95		517	517.6±2.0
0^-, 1	1225.7±6.5	1251.0±7.0	1244	1256±14
	$\Gamma_p(E_R)$ (keV)			
1^-, 1	37.14±0.98	37.07	37	37.4±3.1
0^-, 1	408.57	440±8	416	468±28

Table 4. Radiative widths used in the present calculation along with those from refs. [6,8].

		$\Gamma_\gamma(E_R)$ (eV)		
J^π, T	J^π, E_f	Ref. [6]	Ref. [8]	Present
1^-, 1	1^+, 0.00	9.1±1.3	9.1	9.1±0.6
	0^+, 2.31	0.22±0.04	0.22	0.22±0.05
	1^+, 3.95	1.53±0.21	1.53	1.57±0.07
	0^-, 4.92	0.262±0.043	0.26	0.27±0.03
	2^-, 5.11	0.075±0.025	0.085	0.074±0.019
	1^-, 5.69	0.61±0.14	0.63	0.61±0.08
0^-, 1	1^+, 0.00	46±12	56	40.3±1.8

Table 5. Comparison of $S(0)$ values derived in this work and the previous ones from refs. [8,14,9].

State ^{14}N	$S(0)$ (kev·b)			
J_f^π, E_f	Ref. [8]	Ref. [14]	Ref. [9]	Present
1^+, 0.00	5.16±0.72	5.06	3.54±0.59	5.78±0.48
0^+, 2.31	0.32±0.08	0.35		0.42±0.06
1^+, 3.95	0.90±0.13	0.79		0.90±0.06
0^-, 4.92	0.33±0.07	0.17		0.20±0.01
2^-, 5.11	0.046±0.009	0.046		0.030±0.004
1^-, 5.69	0.77±0.09	0.5		0.56±0.04
3^-, 5.83	0.031±0.007	0.03		0.029±0.003
Total	7.58±1.10	6.94	4.85±0.76	7.92±0.49

where i is the resonance number, $\delta = \arctan\left[\frac{\Gamma_p(E)}{2(E-E_R)}\right]$ denotes the resonance phase shift. The sign of interference term has to be determined experimentally. For the $s \rightarrow p$ direct capture transition, the cross-section has been observed to interfere constructively with the resonant cross-section below the resonance and destructively above it [36]. Tang *et al.* found the same interfere pattern using an R-matrix method [37].

Among the direct measurements of $^{13}C(p,\gamma)^{14}N_0$ reaction, only Zeps *et al.* [38] provided the available excitation function which covered both the 1^- and 0^- resonances. However, a thicker target was adopted in the experiment, and thus the energy divergence is too large to derive the resonance parameters at low energies around 1^- resonance. We have transformed the excitation function reported in ref. [38] to astrophysical $S(E)$ factors through normalizing to the data of 1^- resonance peak [6,9], and the result is well consistent with that from ref. [6] in the energy range of 600–900 keV. Consequently, we chose the data of 100–900 keV from ref. [6] together with those of 600–1850 keV from ref. [38] as a benchmark for the following analysis.

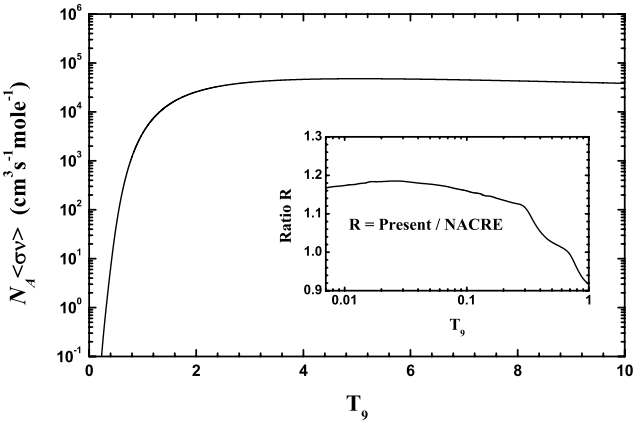

Fig. 6. Astrophysical $^{13}C(p,\gamma)^{14}N$ reaction rates of present work, and the inset is the ratio of our adopted reaction rates to the reaction rates adopted in the NACRE compilation.

Table 6. Fitting parameters of the astrophysical $^{13}C(p,\gamma)^{14}N$ reaction rates.

Parameters	Values	Parameters	Values
a_0	52.6082	b_0	10.5173
a_1	−0.926046	b_1	0.00187505
a_2	−79.2444	b_2	−14.7077
a_3	35.0371	b_3	12.0486
a_4	0.971640	b_4	−1.85193
a_5	−0.371766	b_5	0.127750
a_6	−35.0429	b_6	−2.82447

In the previous studies [6,8], only 1^- resonance data were used in deriving both the 1^- and 0^- resonant parameters, and the component of direct capture was taken as an adjustable parameter. The experimental data of 1^- resonance can be reproduced successfully by using our $S_{dc}(E)$ factors and their resonant parameters, whereas those of 0^- resonance clearly deviate from the calculation. Because of the considerable influences from the high energy tail of 1^- resonance as well as from the direct capture component on the 0^- resonance, it is necessary to fit experimental $S(E)$ factors involving both the 1^- and 0^- resonances for redetermining the parameters of these two resonances, and then extrapolating the $S(E)$ factors.

In what follows, the experimental $S(E)$ factors chosen above were fitted with eq. (8) to determine the 1^- and 0^- resonance parameters as well as to extrapolate the $S(E)$ factors on the basis of our new indirect determination of the $S_{dc}(E)$ factors. The extracted resonance parameters are listed in tables 3 and 4 together with the previous ones. With the new resonance parameters, the astrophysical $^{13}C(p,\gamma)^{14}N_0$ $S(E)$ factors are computed over the energy range of 0–2 MeV, as shown with solid line in fig. 5, and the upper and lower limits are estimated with the errors of spectroscopic factor, direct measurement data and fitting result. As can be seen from fig. 5, the low-energy tail of 1^- resonance and its interference with the direct capture dominates the $S(0)$ factor, and those of 0^- res-

onance also make a considerable contribution ($\sim$ 21%). On the other hand, the high-energy tail of 1^- resonance affects the determination of the 0^- resonance parameters significantly, and therefore does the value of $S(0)$ factor. Thus it is more reasonable to take the direct measurement data of these two resonances into account in the extrapolation of $S(E)$ factors.

The total astrophysical ^{13}C$(p,\gamma)^{14}$N $S(E)$ factors are the sum of the individual ones for the transitions to the ground and first six excited states. Following the above procedure, the $S_{^{14}\mathrm{N}^*_1}$ from this work and the $S_{^{14}\mathrm{N}^*_{2\sim6}}$ from refs. [8,13,16] were used to calculate the $S_{\mathrm{dc}}(E)$ factors for the first and other excited states, respectively. The ^{13}C$(p,\ \gamma)^{14}\mathrm{N}^*_{1\sim6}$ direct measurement data from King *et al.* [6] along with the current E_{R} and $\Gamma_p(E_{\mathrm{R}})$ were used for updating the radiative widths. The results are also listed in table '4. The calculated $S(0)$ values corresponding to the ground and individual excited states as well as the total are listed in table 5. The total $S(25\,\mathrm{keV})$ is found to be 8.20 ± 0.51 keV b.

The astrophysical ^{13}C$(p,\gamma)^{14}$N reaction rates are calculated with

$$N_A\langle\sigma\nu\rangle = N_A\left(\frac{8}{\pi\mu}\right)^{1/2}\frac{1}{(k_BT)^{3/2}} \times \int_0^\infty S(E)\exp\left[-2\pi\eta - \frac{E}{k_BT}\right]\mathrm{d}E, \quad (9)$$

where ν is the relative velocity of the colliding nuclei, N_A and k_B are Avogadro and Boltzmann constants, respectively. Our reaction rates are shown in fig. 6, along with the ratios of ours to the adopted ones in the NACRE compilation [39]. It can be seen that ours are a factor of 1.18 higher at temperatures corresponding to hydrostatic hydrogen burning.

The total reaction rates as a function of temperature obtained in this work are parameterized with an expression used in the REACLIB [40],

$$\begin{aligned} N_A\langle\sigma\nu\rangle = \exp(&a_0 + a_1T_9^{-1} + a_2T_9^{-1/3} + a_3T_9^{1/3} + a_4T_9 \\ &+a_5T_9^{5/3} + a_6\ln T_9) + \exp(b_0 + b_1T_9^{-1} \\ &+b_2T_9^{-1/3} + b_3T_9^{1/3} + b_4T_9 \\ &+b_5T_9^{5/3} + b_6\ln T_9). \end{aligned} \quad (10)$$

The values of fit parameters $a_{0\sim6}$ and $b_{0\sim6}$ for the present adopted reaction rates are listed in table 6, and the fitting errors are less than 2% in the temperature range of $0.001 < T_9 < 10$.

5 Summary and discussion

In this work the angular distributions of the ^{7}Li + ^{13}C elastic scattering and the ^{13}C(^{7}Li, ^{6}He)$^{14}\mathrm{N}_{0,1}$ reactions have been measured at $E(^7\mathrm{Li}) = 34$ MeV with the Q3D magnetic spectrometer. The first peaks of angular distributions for the transfer reactions have been completely presented for the first time. The data were fairly reproduced by the DWBA calculations, and then the proton spectroscopic factors of $^{14}\mathrm{N}_0$ and $^{14}\mathrm{N}^*_1$ were derived.

The ^{13}C$(p,\gamma)^{14}$N direct capture $S_{\mathrm{dc}}(E)$ factors were determined by using the proton spectroscopic factors of ^{14}N. Based on our new indirect determination of the $S_{\mathrm{dc}}(E)$ factors, the direct measurement data of both the 1^- and 0^- resonances were well fitted with the updated resonant parameters, and then the astrophysical ^{13}C$(p,\gamma)^{14}$N $S(E)$ factors were extrapolated over the energy range of 0–2 MeV. The result indicates that these two resonances should be taken into account simultaneously for the precise analysis of $S(E)$ factors.

The astrophysical ^{13}C$(p,\gamma)^{14}$N reaction rates derived in this work are a factor of 1.18 higher than the adopted in NACRE compilation for the temperature range of hydrostatic hydrogen burning. This may change the ^{13}C stellar abundance and thus the ratio of ^{12}C to ^{13}C as well as slightly weaken the ^{13}C$(\alpha,\ n)^{16}$O reaction as a neutron source for the *s* process. The present work offers an independent examination to the existing results of the ^{13}C$(p,\gamma)^{14}$N reaction.

The authors wish to thank Prof. Y.S. Chen and Prof. N.C. Shu for useful discussion, and the referees for their helpful comments to improve the manuscript. This work is supported by the National Natural Science Foundation of China under Grant Nos. 11021504, 10720101076, 10735100 and 10975193, the National Basic Research Program of China under Grant No. 2007CB815003.

References

1. C.E. Rolfs, W.S. Rodney, *Cauldrons in the Cosmos* (The University of Chicago Press, Chicago, 1988) p. 365.
2. M. Lugaro, F. Herwig, J.C. Lattanzio, R. Gallino, O. Straniero, Astrophys. J. **586**, 1305 (2003).
3. E.J. Woodbury, W.A. Fowler, Phys. Rev. **85**, 51 (1952).
4. D.F. Hebbard, J.L. Vogl, Nucl. Phys. **21**, 652 (1960).
5. R.E. Hester, W.A.S. Lamb, Phys. Rev. **121**, 584 (1961).
6. J.D. King, R.E. Azuma, J.B. Vise, J. Görres, C. Rolfs, H.P. Trautvetter, A.E. Vlieks, Nucl. Phys. A **567**, 354 (1994).
7. A.M. Mukhamedzhanov, A. Azhari, V. Burjan, C.A. Gagliardi, V. Kroha, A. Sattarov, X. Tang, L. Trache, R.E. Tribble, Phys. Rev. C **66**, 207602 (2002).
8. A.M. Mukhamedzhanov, A. Azhari, V. Burjan, C.A. Gagliardi, V. Kroha, A. Sattarov, X. Tang, L. Trache, R.E. Tribble, Nucl. Phys. A **725**, 279 (2003).
9. G. Genard, P. Descouvemont, G. Terwagne, J. Phys. Conf. Ser. **202**, 012015 (2010).
10. G.S. Mutchler, D. Rendic, D.E. Velkley, W.E. Sweeney, G.C. Phillips, Nucl. Phys. A **172**, 469 (1971).
11. J.R. Bobbitt, M.P. Etten, G.H. Lenz, Nucl. Phys. A **203**, 353 (1973).
12. R.J. Peterson, J.J. Hamill, Nucl. Phys. A **362**, 163 (1981).
13. P. Bém, V. Burjan, V. Kroha, J. Novák, Š. Piskoř, E. Šimečková, J. Vincour, C.A. Gagliardi, A.M. Mukhamedzhanov, R.E. Tribble, Phys. Rev. C **62**, 024320 (2000).

14. S.V. Artemov, A.G. Bajajin, S.B. Igamov, S.B. Igamov, G.K. Nie, R. Yarmukhamedov, Phys. At. Nucl. **71**, 998 (2008).
15. J. Cook, M.N. Stephens, K.W. Kemper, Nucl. Phys. A **466**, 168 (1987).
16. L. Trache, A. Azhari, H.L. Clark, C.A. Gagliardi, Y.W. Lui, A.M. Mukhamedzhanov, R.E. Tribble, F. Carstoiu, Phys. Rev. C **58**, 2715 (1998).
17. K.W. Kemper, R.L. White, L.A. Charlton, G.D. Gunn, G.E. Moore, Phys. Lett. B **52**, 179 (1974).
18. L. Lapikás, J. Wesseling, R.B. Wiringa, Phys. Rev. Lett. **82**, 4404 (1999).
19. Z.H. Li, E.T. Li, B. Guo, X.X. Bai, Y.J. Li, S.Q. Yan, Y.B. Wang, G. Lian, J. Su, B.X. Wang, S. Zeng, X. Fang, W.P. Liu, Eur. Phys. J. A **44**, 1 (2010).
20. Z. Li, Y. Cheng, C. Yan, J. Yang, Q. Zhang, S. Li, K. Zhao, X. Lu, C. Jiang, Nucl. Instrum. Methods Phys. Res. A **336**, 150 (1993).
21. I.J. Thompson, Comput. Phys. Rep. **7**, 167 (1998).
22. K.O. Groeneveld, A. Richter, U. Strohbusch, B. Zeidman, Phys. Rev. Lett. **27**, 1806 (1971).
23. G. Bassani, N. Saunier, B.M. Traore, J. Raynal, A. Foti, G. Pappalardo, Nucl. Phys. A **189**, 353 (1972).
24. S. Cohen, D. Kurath, Nucl. Phys. **73**, 1 (1965).
25. S. Cohen, D. Kurath, Nucl. Phys. A **101**, 1 (1967).
26. N.K. Timofeyuk, Phys. Rev. C **81**, 064306 (2010).
27. D.J. Millener, *in Topics in Strangeness Nuclear Physics* edited by P. Bydzovsky, A. Gal, J. Mares, in Lect. Notes Nucl. Phys., Vol. **724** (Springer, New York, 2007) p. 31.
28. Z.H. Li, W.P. Liu, X.X. Bai, B. Guo, G. Lian, S.Q. Yan, B.X. Wang, S. Zeng, Y. Lu, J. Su, Y.S. Chen, K.S. Wu, N.C. Shu, T. Kajino, Phys. Rev. C **71**, 052801(R) (2005).
29. Z.H. Li, B. Guo, S.Q. Yan, G. Lian, X.X. Bai, Y.B. Wang, S. Zeng, J. Su, B.X. Wang, W.P. Liu, N.C. Shu, Y.S. Chen, H.W. Chang, L.Y. Jiang, Phys. Rev. C **74**, 035801 (2006).
30. J. Su, Z.H. Li, B. Guo, W.P. Liu, X.X. Bai, S. Zeng, G. Lian, S.Q. Yan, B.X. Wang, Y.B. Wang, Chin. Phys. Lett. **23**, 55 (2006).
31. J. Su, Z.H. Li, B. Guo, X.X. Bai, Z.C. Li, J.C. Liu, Y.B. Wang, G. Lian, S. Zeng, B.X. Wang, S.Q. Yan, Y.J. Li, E.T. Li, Q.W. Fan, W.P. Liu, Chin. Phys. Lett. **27**, 052101 (2010).
32. O. Camargo, V. Guimarães, R. Lichtenthäler, V. Scarduelli, J.J. Kolata, C.A. Bertulani, H. Amro, F.D. Becchetti, J. Hao, E.F. Aguilera, D. Lizcano, E. Martinez-Quiroz, H. Garcia, Phys. Rev. C **78**, 034605 (2008).
33. J. Görres, S. Graff, M. Wiescher, R.E. Azuma, C.A. Barnes, H.W. Becker, T.R. Wang, Nucl. Phys. A **517**, 329 (1990).
34. A.M. Lane, R.G. Thomas, Rev. Mod. Phys. **30**, 257 (1958).
35. C.E. Rolfs, R.E. Azuma, Nucl. Phys. A **227**, 291 (1974).
36. G.J. Mathews, F.S. Dietrich, Astrophys. J. **287**, 969 (1984).
37. X.D. Tang, A. Azhari, C.A. Gagliardi, A.M. Mukhamedzhanov, F. Pirlepesov, L. Trache, R.E. Tribble, V. Burjan, V. Kroha, F. Carstoiu, Phys. Rev. C **67**, 015804 (2003).
38. V.J. Zeps, E.G. Adelberger, A. Garcia, C.A. Gossett, H.E. Swanson, W. Haeberli, P.A. Quin, J. Sromicki, Phys. Rev. C **51**, 1494 (1995).
39. C. Angulo, M.Arnould, M. Rayet, P. Descouvemont, D. Baye, C. Leclercq-Willain, A. Coc, S. Barhoumi, P. Aguer, C. Rolfs, R. Kunz, J.W. Hammer, A. Mayer, T. Paradellis, S. Kossionides, C. Chronidou, K. Spyrou, S. Degl'Innocenti, G. Fiorentini, B. Ricci, S. Zavatarelli, C. Providencia, H. Wolters, J. Soares, C. Grama, J. Rahighi, A. Shotter, M.L. Rachti, Nucl. Phys. A **656**, 3 (1999).
40. T.K. Thielemann, M. Arnould, J. Truran, in *Advances in Nuclear Astrophysics*, edited by E. Vangioni-Flam, J. Audouze, M. Cassé *et al.* (Editons Frontiers, Gif-sur-Yvette, France, 1987).